Distributionally Robust Weighted k-Nearest Neighbors

Shixiang Zhu
Carnegie Mellon University
shixianz@andrew.cmu.edu

Liyan Xie
The Chinese University of Hong Kong, Shenzhen
xieliyan@cuhk.edu.cn

Minghe Zhang
Georgia Institute of Technology
minghe_zhang@gatech.edu

Rui Gao
University of Texas at Austin
rui.gao@mccombs.utexas.edu

Yao Xie
Georgia Institute of Technology
yao.xie@isye.gatech.edu

Abstract

Learning a robust classifier from a few samples remains a key challenge in machine learning. A major thrust of research has been focused on developing k-nearest neighbor (k-NN) based algorithms combined with metric learning that captures similarities between samples. When the samples are limited, robustness is especially crucial to ensure the generalization capability of the classifier. In this paper, we study a minimax distributionally robust formulation of weighted k-nearest neighbors, which aims to find the optimal weighted k-NN classifiers that hedge against feature uncertainties. We develop an algorithm, `Dr.k-NN`, that efficiently solves this functional optimization problem and features in assigning minimax optimal weights to training samples when performing classification. These weights are class-dependent, and are determined by the similarities of sample features under the least favorable scenarios. The proposed framework can be shown to be equivalent to a Lipschitz norm regularization problem. We also couple our framework with neural-network-based feature embedding. We demonstrate the competitive performance of our algorithm compared to the state-of-the-art in the few-training-sample setting with various real-data experiments.

1 Introduction

Machine learning has been proven successful in data-intensive applications but is often hampered when the data set is small. For example, in breast mammography diagnosis for breast cancer screening [5], the diagnosis of the type of breast cancer requires specialized analysis by pathologists in a highly time- and cost-consuming task and often leads to non-consensual results. As a result, labeled data in digital pathology are generally very scarce; so do many other applications.

In this paper, we aim to tackle the general multi-class classification problem when only very few training samples are available for each class [43]. Evidently, k-Nearest Neighbor (k-NN) algorithm [3] is a natural idea to tackle this problem and shows promising empirical performances. Notable contributions, including seminal work [19] and the follow-up non-linear version [34], go beyond the vanilla k-NN and propose neighborhood component analysis (NCA). NCA learns a distance metric that minimizes the expected leave-one-out classification error on the training data using a stochastic neighbor selection rule. Some recent studies in few-shot learning utilize the limited training data using a similar idea, such as matching network [41] and prototypical network [39]. They are primarily based on distance-weighted k-NN, which classifies an unseen sample (aka. *query*) by a weighted

36th Conference on Neural Information Processing Systems (NeurIPS 2022).

Figure 1: Motivating example: a small training set of three image-label pairs: the first image is a mop; the second image is a dog; the third image looks like a mop but is, in fact, a dog (dressing up as a mop). The query (the last image) is "closer" to the third one and more likely to be misclassified as a dog if we use distance-weighted k-NN.

vote of its neighbors and uses the distance between two data points in the embedding space as their weights.

The classification performance of weighted k-NN critically depends on the choice of weighting scheme. The distance measuring the similarity between samples is typically chosen by metric learning, where a task-specific distance metric is automatically constructed from supervised data [24, 33, 41]. However, it has been recognized that they may be not robust to the *few-training-samples* scenario, where an "outlier" may greatly deteriorate the performance. An example to illustrate this issue is shown in Figure 1. The training set with only three labeled samples includes two categories we want to classify: mop and Komondor. As we can see, the query image is visually closer to the third sample and thus more likely to be misclassified as a Komondor. Here the third sample in the training set is an "outlier", since it is a Komondor dressing up as a mop, and it misleads the metric learning model to capture irrelevant details (e.g., the bucket and the mop handle) for the Komondor category. Such a problem can become even severe when the sample size is small.

The discussion above highlights the importance of choosing a good weighting scheme in weighted k-NN. To develop algorithms that are more robust in the few-training-samples settings, we propose a new formulation of distributionally robust weighted k-nearest neighbors. More specifically, for a given set of features of training samples, we solve a Wasserstein distributionally robust optimization problem that finds the minimax optimal weight functions for the k-nearest neighbors. This infinite-dimensional functional optimization over weight functions presents a unique challenge for which existing literature on distributionally robust optimization do not consider. To tackle this challenge, we first consider a relaxed problem that optimizes over all randomized classifiers, which turns out to admit a finite-dimensional convex programming reformulation in spite of being infinite-dimensional (Theorem 1). Next, we show that there is a weighted k-NN classifier achieving the same risk and shares the same least favorable distributions (LFDs) as the robust classifier (Theorem 2). Thereby we prove the optimality of such weighted k-NN classifier for the original distributionally robust weighted k-nearest neighbors problem. Furthermore, we prove the equivalence between the proposed robust weighted k-NN classifier with a Lipschitz norm regularization problem (Theorem 3), which provides promising insights on the generalization property of the robust classifier.

Based on these theoretical results, we proposed a novel algorithm called `Dr.k-NN`. Unlike the traditional distance-weighted k-NN that uses the same weight for all label classes, our algorithm introduces a vector of weights, one for each class, for each sample in k-NN and performs a weighted majority vote. These weights are determined from the LFDs and reveal the significance of each sample in the worst case, thereby contributing effectively to final decision making. An example is illustrated in Figure 2. Further, using differentiable optimization [4, 2], we incorporate a neural network into the minimax classifier that jointly learns the feature embedding and the minimax optimal classifier. Numerical experiments show that our algorithm can effectively improve the multi-class classification performance with few training samples on various data sets.

Related work Recently, there has been much interest in multi-class classification with few training samples, see [31, 43] for a survey. The main idea of our work is related to metric learning [19, 22, 33, 34, 32], which essentially translates the hidden information carried by the limited data into a distance metric, and has been widely adopted in few-shot learning and meta learning [15, 24, 39, 41, 30]. However, unlike few-shot and meta learning, where the goal is to acquire meta knowledge from a

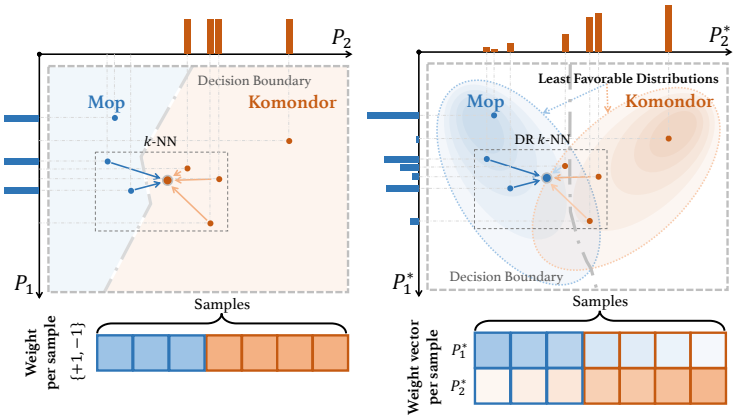

(a) Vanilla k-NN (b) `Dr.k-NN`

Figure 2: An illustrative comparison of `Dr.k-NN` and vanilla k-NN. Each colored dot is a training sample, where the color indicates its class-membership. The horizontal/vertical bar represents the probability mass of one training sample under the distribution P_1, P_2, respectively.

large number of observed classes and then predict examples from unobserved classes, we focus on attacking a specific general classification problem where the number of categories is fixed but labeled data are scarce. In this paper, we take a different probabilistic approach to exploit information from the data: we construct an uncertainty set for distributions of each class based on the Wasserstein distance.

Wasserstein distributionally robust optimization [10, 7, 13, 1, 8, 17, 38, 6, 36, 16] is an emerging paradigm for statistical learning; see [26] for a recent survey. Our work is mostly related to [18], a framework for Wasserstein robust hypothesis testing, but is different in three important ways. First, we focus on multi-class classification, while [18] only studied two hypotheses. Second, we focus on directly minimizing the mis-classification error while [18] used a convex relaxation for the 0-1 loss. Third, we analyze the generalization bound while [18] does not. Fourth, while [18] requires sample features as an input, we develop a scalable algorithmic framework to simultaneously learn the optimal feature extractor parameterized by neural networks and robust classifier to achieve the best performance. A recent work [9] studies distributionally robust k-NN regression. Note that regression and classification are fundamentally different as different performance metrics are used. In [9] the objective is to minimize the mean square error, whereas in our work we minimize classification errors. Last but not least, our minimax formulation is similar to [14], which introduces a generalization of the maximum entropy principle and aims to address a different supervised learning problem. It is worth noting that the paper considers another type of ambiguity set defined via cross-moment constraints. In contrast, we adopt Wasserstein sets in our formulation, leading to different tractable optimization reformulations and regularization terms.

Another well-known work on optimal weighted nearest neighbor binary classifier [35] assigns one weight to each sample; the optimal weights minimize asymptotic expansion for the excess risk (regret). In contrast, we consider minimax robust multi-class classification, each training sample is associated with different weights for different classes, and we consider the few sample regime instead of the asymptotic regime in [35].

2 Distributionally Robust k-NN

In this section, we present our model. We first define weighted k-NN classifier in Section 2.1, then present the proposed framework of distributionally robust k-NN problem in Section 2.2.

2.1 Weighted k-NN classifier

Let $\{(x^1, y^1), \ldots, (x^n, y^n)\}$ be a set of training samples, where x^i denotes the i-th data sample in the observation space $\mathcal{X}$, and $y^i \in \mathcal{Y} := \{1, \ldots, M\}$ denotes the class (label) of the i-th data sample. Let $\phi : \mathcal{X} \to \Xi$ be a feature extractor that embeds samples to the feature space Ξ (in Section 4.2 we will train a neural network to learn ϕ). Denote the sample feature vectors and the empirical support

as:

$$\xi^i := \phi(x^i),\ i = 1, \ldots, n, \quad \widehat{\Xi} := \{\xi^1, \ldots, \xi^n\}.$$

Let

$$S = \{(\xi^1, y^1), \ldots, (\xi^n, y^n)\}.$$

Define empirical distributions:

$$\widehat{P}_m := \frac{1}{|\{i : y^i = m\}|} \sum_{i=1}^{n} \delta_{\xi^i} \mathbb{I}\{y^i = m\},\ m = 1, \ldots, M,$$

where δ denotes the Dirac point mass, $|\cdot|$ denotes the cardinality of a set, and $\mathbb{I}$ denotes the indicator function.

Let $\pi : \Xi \to \Delta_M$ be a *randomized* classifier that assigns class $m \in \{1, \ldots, M\}$ with probability $\pi_m(\xi)$ to a query feature vector $\xi \in \Xi$, where Δ_M is the probabilistic simplex $\Delta_M = \{\pi \in \mathbb{R}_+^M : \sum_{m=1}^M \pi_m = 1\}$. It is worth mentioning that the randomized test is more general than the commonly seen deterministic test. In particular, the random classifier π reduces to the deterministic test if for any ξ, there exists a m such that $\pi_m(\xi) = 1$. Suppose the features in each class m follows a distribution P_m. We define the *risk* of a classifier π as the total error probabilities[1]

$$\Psi(\pi; P_1, \ldots, P_M) := \sum_{m=1}^{M} \mathbb{E}_{\xi \sim P_m}[1 - \pi_m(\xi)]. \tag{1}$$

Recall that the vanilla k-NN is performed as follows. Let $c : \Xi \times \Xi \to \mathbb{R}_+$ be a metric on Ξ that measures distance between features. For any given query point ξ, let $\tau_1^S(\xi), \ldots, \tau_n^S(\xi)$ be a reordering of $\{1, \ldots, n\}$ according to their distance to ξ, i.e., $c(\xi, \xi^{\tau_i^S(\xi)}) \leq c(\xi, \xi^{\tau_{i+1}^S(\xi)})$ for all $i < n$, where the tie is broken arbitrarily. Here the superscript S indicates the dependence on the sample S. In vanilla k-NN, we compute the votes as

$$p_m(\xi) := \sum_{i=1}^{k} \frac{1}{k} \mathbb{I}\{y^{\tau_i^S(\xi)} = m\},\ m = 1, \ldots, M. \tag{2}$$

The vanilla k-NN decides the class for ξ by the majority vote, i.e., accept the class $\arg\max_{1 \leq m \leq M} p_m(\xi)$.

To define a weighted k-NN, let us replace the equal weights in (2) by an arbitrary weight function $w_m : \Xi \times \Xi \to \mathbb{R}_+$ for each class $m = 1, \ldots, M$:

$$p_m(\xi) := \sum_{i=1}^{k} w_m(\xi, \xi^{\tau_i^S(\xi)}), \tag{3}$$

and use a shorthand notation $w := (w_1, \ldots, w_M)$. In the sequel, we define a general tie-breaking rule as follows. For any ξ, denote $\mathcal{M}_0(\xi) := \arg\max_{1 \leq m \leq M}\ p_m(\xi)$. When $|\mathcal{M}_0(\xi)| > 1$, there is a tie at ξ. We denote $\pi_m(\xi)$ as the probability of accepting class m for $m \in \mathcal{M}_0(\xi)$ and we have $\sum_{m \in \mathcal{M}_0(\xi)} \pi_m(\xi) = 1$.

We define a *weighted k-NN classifier* $\pi^{\mathsf{knn}}(\xi; k, w) : \Xi \to \Delta_M$ as:

$$\pi_m^{\mathsf{knn}}(\xi; k, w) = \begin{cases} \pi_m(\xi), & m \in \mathcal{M}_0(\xi), \\ 0, & \text{otherwise.} \end{cases} \tag{4}$$

A weighted k-NN classifier involves two parameters: number of nearest neighbors k and weighting scheme w. Particularly, $w_m(\xi, \xi^i) = \mathbb{I}\{y^i = m\}$ recovers the vanilla k-NN, and $w_m(\xi, \xi^i) = \mathbb{I}\{y^i = m\}/c(\xi, \xi^i)$ recovers the distance-based weighted k-NN. Note that our definition (3) allows different weighting schemes for different classes, which is more general than the standard weighted k-NN.

The goal is to find the optimal weighted k-NN classifier $\pi^{\mathsf{knn}}(\cdot; k, w)$ such that the risk Ψ as defined in (1) is minimized. Since the underlying true distributions are unknown, the commonly used loss

[1] To ease the exposition we consider only equal weights over the error probabilities, but our results can be easily generalized to any weighted average of error probabilities.

function is the empirical loss, i.e., substitute the empirical distributions $\widehat{P}_m$ into the risk function (1). This leads to the following optimization problem:

$$\min_{\substack{1\le k\le n \\ w_m:\Xi\times\Xi\to\mathbb{R}_+,\, 1\le m\le M}} \Psi(\pi^{\mathsf{knn}}(\cdot;k,w);\widehat{P}_1,\ldots,\widehat{P}_M). \tag{5}$$

It is worth mentioning that this minimization problem is an *infinite-dimensional* functional optimization, since the weighting schemes w is a function on $\Xi\times\Xi$.

2.2 Distributionally robust k-NN

For few-training-sample setting, the empirical distributions might not be good estimates for the true distribution since the sample size is small. To hedge against distributional uncertainty, we propose a distributionally robust counterpart of the weighted k-NN problem defined in the previous subsection. Specifically, suppose each class m is associated with a distributional uncertainty set $\mathcal{P}_m$, which will be specified shortly. Given $\mathcal{P}_1,\ldots,\mathcal{P}_M$, define the *worst-case risk* of a classifier π as the worst-case total error probabilities

$$\max_{P_m\in\mathcal{P}_m, 1\le m\le M} \Psi(\pi;P_1,\ldots,P_M),$$

where Ψ is defined in (1).

We consider the following distributionally robust k-NN problem that finds the optimal weighted k-NN classifier minimizing the worst-case risk:

$$\min_{\substack{1\le k\le n \\ w_m:\widehat{\Xi}\times\widehat{\Xi}\to\mathbb{R}_+ \\ 1\le m\le M}} \max_{\substack{P_m\in\mathcal{P}_m \\ 1\le m\le M}} \Psi(\pi^{\mathsf{knn}}(\cdot;k,w);P_1,\ldots,P_M). \tag{6}$$

Here the optimal solution $P_1^*,\ldots,P_M^*$ to the inner maximization problem is also called *least favorable distributions (LFD)* in statistics literature [21]. We summarize the architecture of the proposed distributionally robust k-NN framework in Figure 3, more details are provided in Section 4.

Now we describe the uncertainty set $\mathcal{P}_m$. First, since we are going to re-weight the training samples to build the classifier, we restrict the support of every distribution in $\mathcal{P}_m$ to $\widehat{\Xi}$, the set of empirical points. Second, the uncertainty set is data-driven, containing the empirical distribution $\widehat{P}_m$ and distributions surrounding its neighborhood. Third, to measure the closeness between distributions, we choose the Wasserstein metric of order 1 [40], defined as

$$\mathcal{W}(P,P') := \min_{\gamma}\ \mathbb{E}_{(\xi,\xi')\sim\gamma}\left[c(\xi,\xi')\right]$$

for any two distributions P and P' on Ξ, where the minimization of γ is taken over the set of all probability distributions on $\Xi\times\Xi$ with marginals P and P'. The main advantage of using Wasserstein metric is that it takes account of the *geometry* of the feature space by incorporating the metric $c(\cdot,\cdot)$ in its definition. Given the empirical distribution $\widehat{P}_m$ for $m=1,\ldots M$, we define

$$\mathcal{P}_m := \left\{P_m\in\mathscr{P}(\widehat{\Xi}):\ \mathcal{W}(P_m,\widehat{P}_m)\le\vartheta_m\right\}, \tag{7}$$

where $\mathscr{P}(\widehat{\Xi})$ denotes the set of all probability distributions on $\widehat{\Xi}$; $\vartheta_m\ge 0$ specifies the size of the uncertainty set for the m-th class that specifies the amount of deviation we would like to control.

3 Theoretical Properties

In this section, we analyze the computational tractability and statistical properties of the proposed distributionally robust weighted k-NN classifier found in (6). All proofs are delegated to Appendix B.

3.1 Robust Classification

Observe that similar to (5), the formulation (6) is also an infinite-dimensional functional optimization. Let us first relate it to a relaxed robust classification problem, which turns out to be more tractable.

Consider the following minimax robust classification problem over all randomized classifiers π (recalling Δ_M is the probability simplex in $\mathbb{R}_+^M$):

$$\min_{\pi:\Xi\to\Delta_M}\ \max_{P_m\in\mathcal{P}_m, 1\le m\le M} \Psi(\pi;P_1,\ldots,P_M). \tag{8}$$

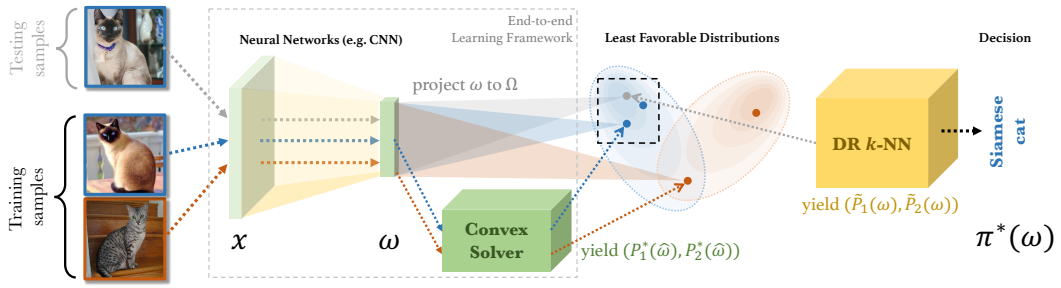

Figure 3: An overview of the end-to-end learning framework, which consists of two cohesive components: (1) an architecture that is able to produce feature embedding ξ and least favorable distributions P_m^* for training set; (2) an `Dr.k-NN` makes decisions for any unseen sample ξ based on the estimated weight vector $\widetilde{p}_m(\xi)$ (probability mass on least favorable distributions).

Yet still, (8) is an infinite-dimensional functional optimization, since we are optimizing over the set of all randomized classifiers. We establish the following theorem stating a finite-dimensional convex programming reformulation for the problem (8).

Theorem 1. *For the uncertainty sets defined in* (7)*, the least favorable distribution of problem* (8) *can be obtained by solving the following problem:*

$$\begin{aligned} \min_{\substack{p_1,\ldots,p_M\in\mathbb{R}_+^n\\ \gamma_1,\ldots,\gamma_M\in\mathbb{R}_+^{n\times n}}} \quad & \sum_{i=1}^n \max_{1\le m\le M} p_m^i \\ \textit{subject to} \quad & \sum_{i=1}^n\sum_{j=1}^n \gamma_m^{i,j} c(\xi^i,\xi^j) \le \vartheta_m, \\ & \sum_{i=1}^n \gamma_m^{i,j} = \widehat{P}_m(\xi^j), \quad \sum_{j=1}^n \gamma_m^{i,j} = p_m^i, \\ & \forall 1\le i,j\le N,\ 1\le m\le M. \end{aligned} \tag{9}$$

The decision variable $\gamma_m \in \mathbb{R}_+^{n\times n}$ can be viewed as a joint distribution on n empirical points with marginal distributions $\widehat{P}_m$ and P_m, represented by a vector $p_m \in \mathbb{R}_+^n$. The inequality constraint controls the Wasserstein distance between P_m and $\widehat{P}_m$.

Below we give an intuitive explanation for the objective function in (9). Note that $\max_{1\le m'\le M} p_{m'}^i - p_m^i$ measures the margin between the maximum likelihood of ξ^i among all classes and the likelihood of the m-th class. Thus, the objective in (9) can be equivalently rewritten as minimization of total margin:

$$\sum\nolimits_{i=1}^n \sum\nolimits_{m=1}^M \left(\max_{1\le m'\le M} p_{m'}^i - p_m^i \right).$$

When $M=2$, the total margin reduces to the total variation distance. Also, let $y_m^i \in \{0,1\}$ be the class indicator variable of sample ξ^i, observe that

$$\sum_{i=1}^n \max_{1\le m\le M} p_m^i = \lim_{t\to\infty} \left(\sum_{i=1}^n\sum_{m=1}^m y_m^i p_m^i - \frac{1}{t}\sum_{i=1}^n\sum_{m=1}^M y_m^i \log \frac{\exp(tp_m^i)}{\sum_{m=1}^M \exp(tp_m^i)} \right),$$

where the second term on the right side represents the cross-entropy (or negative log-likelihood).

Therefore, problem (9) perturbs $(\widehat{P}_1,\ldots,\widehat{P}_M)$ to LFDs $(P_1^*,\ldots,P_M^*)$ so as to minimize the total margin as well as an upper bound on cross-entropy of LFDs; the smaller the margin (or cross-entropy) is, the more similar between classes and thus the harder to distinguish among them.

3.2 Expressiveness of Weighted k-NN

In this subsection we study the expressive power of the class of weighted k-NN classifiers

$$\{\pi^{\mathsf{knn}}(\cdot;k,w)\colon 1\le k\le n, w_m\colon \Xi\times\Xi\to\mathbb{R}_+, 1\le m\le M\}$$

defined in Section 2.1.

The following theorem establishes the equivalence between the original problem (6) and the relaxed robust classification problem (8) studied in Section 3.1.

Theorem 2. *For the uncertainty set defined in* (7)*, formulations* (6) *and* (8) *have identical optimal values. In addition, there exists optimal solutions of* (6) *and* (8) *that share common LFDs that are optimal to* (9)*.*

Theorem 2 implies that the set of weighted k-NN classifiers is *exhaustive*, in the sense that it achieves the same optimal robust risk as optimizing over the set of all randomized classifiers. In our proof, we show that the *weighted 1-NN classifier*, with weights equal to the LFDs of (9), is an optimal solution to (6). Therefore, instead of solving (6) directly, by Theorem 1, we can solve the convex program (9) for the LFDs, based on which we construct a robust k-NN classifier. This justifies the `Dr.k-NN` algorithm to be described in Section 4.

3.3 Lipschitz Regularization

Next, we discuss the connection between the proposed distributional robust k-NN framework in (6), (8) and an equivalent Lipschitz regularization problem.

Using duality for Wasserstein DRO [17], problem (8) is equivalent to

$$\min_{\substack{\pi:\widehat{\Xi}\to\Delta_M\\ \lambda_m\geq 0, m=1,\ldots M}} \left\{ \sum_{m=1}^{M} \lambda_m \vartheta_m + \mathbb{E}_{\hat{\xi}\sim\widehat{P}_m}\left[\max_{\xi\in\widehat{\Xi}}\left\{1-\pi_m(\xi)-\lambda_m c(\xi,\hat{\xi})\right\}\right]\right\}. \tag{10}$$

Then by [16], this problem is upper bounded by the following Lipschitz regularized classification problem

$$\min_{\pi:\widehat{\Xi}\to\Delta_M} \sum_{m=1}^{M} \left\{ \mathbb{E}_{\xi\sim\widehat{P}_m}\left[1-\pi_m(\xi)\right] + \vartheta_m \|\pi_m\|_{\text{Lip}} \right\}, \tag{11}$$

where

$$\|\pi_m\|_{\text{Lip}} := \max_{\xi,\tilde{\xi}\in\widehat{\Xi},\, \xi\neq\tilde{\xi}} \frac{|\pi_m(\tilde{\xi})-\pi_m(\xi)|}{c(\tilde{\xi},\xi)}$$

is the Lipschitz norm of the function π_m for each $m=1,\ldots,M$. Perhaps surprisingly, the next result shows that (10) and (11) are actually equivalent (thus by Theorem 2, are both equivalent to (6)), despite that the loss function does not satisfy existing criteria ensuring the equivalence [13, 36, 16].

Theorem 3. *Formulations* (10) *and* (11) *are equivalent, and there exists an optimizer* π^* *of* (11) *satisfying* $\|\pi_m^*\|_{\text{Lip}} = \lambda_m^*$*,* $m=1,\ldots,M$*, where* $(\lambda_m^*)_m$ *is the optimizer of* (10) *when* $\pi=\pi^*$*.*

The theorem is proved by using c-transform [40] to show that any optimizer π_m^* can be modified into a λ_m^*-Lipschitz classifier while maintaining the optimality. Note that Lipschitz classifiers are known to enjoy good generalization property [42, 20], thus the equivalence provides promising insights for the generalization property of the robust classifier.

4 Proposed Algorithm `Dr.k-NN`

In this section, we present the Distributional robust k-Nearest Neighbor (`Dr.k-NN`) algorithm, which is a direct consequence of the theoretical justifications in Section 3.

4.1 `Dr.k-NN` algorithm

Based on Theorem 2, our algorithm contains two steps.

Step 1. [*Sample re-weighting*] For each class m, re-weight n samples using a distribution P_m^*, where $(P_1^*,\ldots,P_M^*)$ is the p-component of the minimizer of (9).

Step 2. [*k-NN*] Given a query point ξ, ordering the training samples according to their distance to ξ: $c(\xi,\xi^{\tau_1^S(\xi)}) \leq c(\xi,\xi^{\tau_2^S(\xi)}) \leq \cdots \leq c(\xi,\xi^{\tau_n^S(\xi)})$. Compute the weighted k-NN votes, define

$$\widetilde{p}_m(\xi) := \frac{1}{k}\sum_{i=1}^{k} P_m^*(\xi^{\tau_i^S(\xi)}),\ m=1,\ldots,M. \tag{12}$$

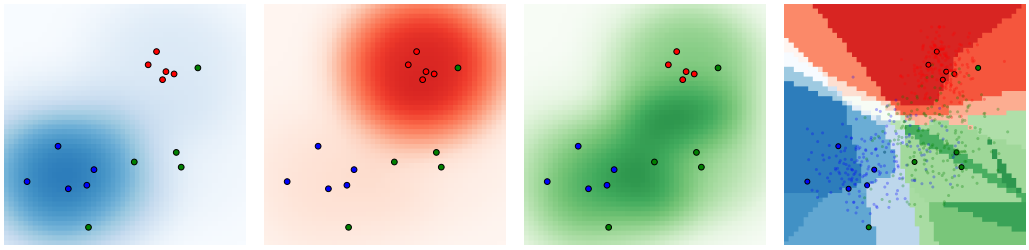

(a) P_1^* (b) P_2^* (c) P_3^* (d) π^*

Figure 4: An example of the weights P_1^*, P_2^*, P_3^* yielding from (9) and the corresponding results of `Dr.k-NN` using a small subset of MNIST (digit 4 (red), 6 (blue), 9 (green) and $k = 5$). Raw samples are projected on a 2D feature space ($d = 2$), with the color indicating their true class-membership. In (a)(b)(c), shaded areas indicate the kernel smoothing of P_1^*, P_2^*, P_3^* defined in (13). In (d), big dots represent the training points and small dots represent the query points, and their color depth suggests how likely the sample is being classified into the true category.

Table 1: Comparison of classification accuracy in the few-training-sample setting

Methods	MNIST				*mini* ImageNet				CIFAR-10				Omniglot				Lung Cancer		COVID-19 CT	
	$M=2$		$M=5$		$M=2$		$M=5$		$M=2$		$M=5$		$M=2$		$M=5$		$M=3$		$M=2$	
	$K=5$	$K=10$	$K=5$	$K=10$	$K=5$	$K=10$	$K=5$	$K=10$	$K=5$	$K=10$	$K=5$	$K=10$	$K=5$	$K=10$	$K=5$	$K=10$	$K=5$	$K=8$	$K=5$	$K=10$
PCA+k-NN	0.801	0.872	0.614	0.678	0.578	0.667	0.268	0.277	0.687	0.711	0.262	0.270	0.597	0.638	0.309	0.358	0.617	0.647	0.658	0.719
SVD+k-NN	0.749	0.790	0.524	0.567	0.587	0.675	0.268	0.283	0.680	0.701	0.259	0.266	0.591	0.618	0.305	0.413	0.624	0.648	0.646	0.715
NCA+k-NN	0.602	0.640	0.340	0.355	0.547	0.578	0.245	0.258	0.597	0.616	0.232	0.236	0.549	0.574	0.267	0.346	0.575	0.582	0.612	0.624
Matching Net	0.732	0.830	0.625	0.732	0.687	0.703	0.286	**0.360**	0.632	0.641	0.241	0.247	0.735	0.769	0.412	0.433	0.621	0.635	0.715	0.732
Prototypical Net	0.742	0.842	0.671	0.759	0.710	0.725	0.296	0.348	0.651	0.664	0.254	0.259	**0.769**	**0.836**	**0.448**	0.532	0.632	0.644	**0.729**	**0.744**
MetaOptNet	0.725	0.843	0.658	0.790	0.732	0.741	0.255	0.363	0.702	0.713	0.257	0.298	0.742	0.755	0.412	0.453	0.638	0.642	0.713	0.739
Feature embedding + k-NN	0.792	0.798	0.546	0.551	0.738	0.742	**0.490**	**0.486**	0.689	0.691	**0.492**	**0.494**	0.725	0.751	0.445	0.495	**0.664**	0.691	0.701	0.710
Kernel Smoothing	0.777	0.873	0.559	0.579	0.593	0.601	0.272	0.278	0.642	0.661	0.272	0.282	0.520	0.565	0.240	0.285	0.367	0.370	0.582	0.604
Truncated Dr.k-NN	**0.815**	**0.926**	**0.742**	**0.825**	**0.746**	**0.753**	0.295	0.340	**0.703**	**0.719**	0.297	0.305	0.755	0.825	0.425	**0.542**	0.652	**0.693**	0.722	0.741
Dr.k-NN	**0.838**	**0.959**	**0.746**	**0.831**	**0.752**	**0.786**	**0.306**	0.358	**0.707**	**0.728**	**0.309**	**0.311**	**0.765**	**0.850**	**0.465**	**0.580**	**0.667**	**0.704**	**0.734**	**0.752**

Decide the class for a query feature point ξ as $\arg\max_{1\le m\le M} \widetilde{p}_m(\xi)$, where the tie is broken according to the rule (4).

Figure 4 gives an illustration showing the probabilistic weights (P_1^*, P_2^*, P_3^*) for three classes and its corresponding decision boundary yielding from the weighted k-NN.

For the sake of completeness, we also extend our algorithm to non-few-training-sample setting, which is referred to as truncated `Dr.k-NN`. The key idea is to keep the training samples that are important in deciding the decision boundary based on the maximum entropy principle [11]. This can be particularly useful for the general classification problem with an arbitrary size of training set. An illustration (Figure 6) and more details can be found in Appendix C.

4.2 Joint learning framework

In this section, we propose a framework that jointly learns the feature mapping and the robust classifier. Let the feature mapping $\phi(;\theta)$ be a neural network parameterized by θ whose input is a batch of training samples (Figure 3), and then compose it with an optimization layer that packs the convex problem (9) as an output layer that outputs the LFDs of (8). The optimization layer is adopted from differentiable optimization [4, 2], in which the optimization problem is integrated as an individual layer in an end-to-end trainable deep networks and the solution of the problem can be backpropagated through neural networks.

To apply the mini-batch stochastic gradient descent, we need to ensure that each batch comprises of multiple "mini-sets", one for each class, containing at least one training sample from each class fed into the convex optimization layer. In light of (9), the objective of our joint learning framework is $\min_\theta J(\theta; P_1^*, \dots, P_M^*)$, where

$$J(\theta; P_1^*, \dots, P_M^*) := \sum_{i=1}^{n} \max_{1\le m\le M} P_m^*(\phi(x^i;\theta)),$$

and $\{P_m^*(\phi(\cdot;\theta))\}_{1\le m\le M}$ are the LFDs generated by the convex solver defined in (9) given input variables $\{\xi^i = \phi(x^i;\theta)\}_{1\le i\le n}$. The algorithm is summarized in Algorithm 1 (Appendix A).

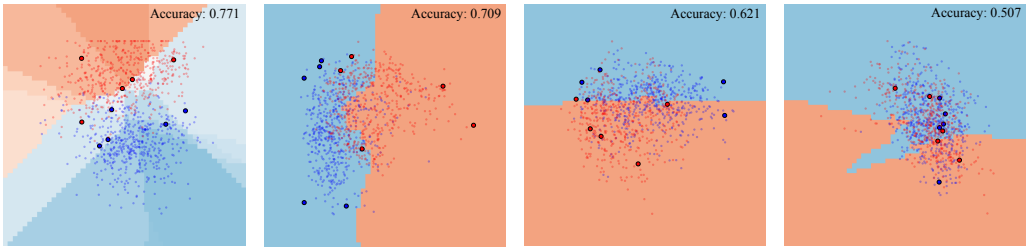

(a) `Dr.k-NN` (b) PCA + k-NN (c) SVD + k-NN (d) NCA.

Figure 5: A comparison of the learned feature spaces and the corresponding decision boundaries. There are 10 training samples from two categories of MNIST identified as large dots and 1,000 query samples identified as small dots. The color of dots shows their true categories. The color of the region shows the decisions made by corresponding methods.

5 Experiments

In this section, we evaluate our method and eight alternative approaches on four commonly-used image data sets: MNIST [28], CIFAR-10 [25], Omniglot [27], and present a set of comprehensive numerical examples.

We also test our method on two medical diagnosis data sets: Lung Cancer [12], and COVID-19 CT [44], where very few data samples are available for study, due to privacy concerns and high costs associated with harvesting data. Specifically, Lung Cancer data record 56 attributes for only 32 patients who have been diagnosed with three types of pathological lung cancers; COVID-19 Computed Tomography (CT) data contain 349 COVID-19 CT images from 216 patients and 463 non-COVID-19 CTs. Here, we present a few examples of COVID-19 CT images and non-COVID-19 CT images in Appendix E.

Experiment set-up. We compare our method including `Dr.k-NN` and its truncated version with the following baselines: (1) k-NN based methods with different dimension reduction techniques, including Principal Component Analysis (`PCA+`k`-NN`), Singular Value Decomposition (`SVD+`k`-NN`), Neighbourhood Components Analysis (`NCA+`k`-NN`) [19], and feature embeddings generated by Dr.k-NN (Feature embedding + k-NN) as a sanity check; (2) matching networks [41]; (3) prototypical networks [39]; (4) MetaOptNet [29]. To make these methods comparable, we adopt the same naive neural network with a single CNN layer on matching network, prototypical network, and our model, respectively, where the kernel size is 3, the stride is 1 and the width of the output layer is $d = 400$.

In our experiments, we focus on an M-class K-sample (K training samples for each class) learning task. To generate the training data set, we randomly select M classes and for each class we take K random samples. So our training data set contains MK samples overall. We then aim to classify a disjoint batch of unseen samples into one of these M classes. Thus random performance on this task stands at $1/M$. We test the average performance of different methods using $1,000$ unseen samples from the same M classes. To obtain reliable results, we repeat each test 10 times and calculate the average accuracy.

Other experimental configurations are described as follows: The Adam optimizer [23] is adopted for all experiments conducted in this paper, where learning rate is 10^{-2}. The mini-batch size is 32. The hyper-parameter ϑ_m is chosen by cross-validation, which varies from application to application. The differentiable convex optimization layer we adopt is from [2]. To make all approaches comparable, we use the same network structure in matching network, prototypical network, and MetaOptNet as we described above. We use the Euclidean distance $c(\xi, \xi') = \|\xi - \xi'\|_2$ throughout our experiment. All experiments are performed on Google Colaboratory (Pro version) with 12GB RAM and dual-core Intel processors, which speed up to 2.3 GHz (without GPU).

Results. We present the average test accuracy in Table 1 for the unseen samples with different $M = 2, 5$ and $K = 5, 10$ on small subsets of MNIST, *mini* ImageNet, CIFAR-10, Omniglot, and with $M = 3$ and $K = 5, 8$ on lung cancer data. Note that random performance for two-class and five-class classifications are 0.5 and 0.2, respectively. The figures in Table 1 show that `Dr.k-NN` ($k = 5$) outperforms other baselines in terms of the average test accuracy on all data sets. We note

that 95% confidence interval of our method's performance on all the data sets is smaller than 0.08. The truncated `Dr.k-NN` also yields competitive results using only 20% training samples ($\tau = 0.9$), compared to standard `Dr.k-NN`.

To confirm that the proposed learning framework will affect the distribution of hidden representation of data points, we show the training and query samples in a 2D feature space and the corresponding decision boundary in Figure 5. It turns out our framework finds a better feature representation in the 2D space with a smooth decision boundary and a reasonable decision confidence map (indicated by the color depth in Figure 5 (a)).

Comparison to kernel smoothing. We also compare with an approach using kernel-smoothing of the LFDs (in contrast to using k-NN) for performing classification. Consider a Gaussian kernel $\kappa(x) = |H_h|^{-1/2}\kappa(H_h^{-1/2}x)$, where $H_h = hI_p$ is the isotropical kernel with bandwidth h. Then we replace $\widetilde{p}_m(\xi)$ in Step 2 of `Dr.k-NN` with the following

$$\widetilde{p}_m(\xi) \coloneqq \sum_{i=1}^{n} P_m^*(\xi^i)\kappa(\xi - \xi^i),\ \forall \xi,\ m = 1, \ldots, M. \tag{13}$$

We evaluate both methods on a subset of MNIST, which contains 1,000 testing samples (small dots) and 20 training samples (large dots) from two categories (indexed by blue and red, respectively).

As shown in Figure 7 and Figure 8 (Appendix D), our experimental results have shown the importance of using k-NN in our proposed algorithm, where the `Dr.kNN` significantly outperforms the parallel version using kernel smoothing (even after the kernel bandwidth being optimized). We find that the performance when using kernel smoothing (13) heavily depends on selecting an appropriate kernel bandwidth h as illustrated by Figure 8.

Moreover, the best kernel bandwidth may vary from one dataset to another. Therefore, the cross-validation is required to be carried out to find the best kernel bandwidth in practice, which is quite time-consuming. In contrast, choosing the hyper-parameter k is an easy task, since we only have limited choices of k in few-training-sample scenario and the performance of `Dr.k-NN` is insensitive to the choices of k (see Figure 7).

6 Conclusion

We propose a distributionally robust k-NN classifier (`Dr.k-NN`) for tackling the multi-class classification problem with few training samples. To make a decision, each neighboring sample is weighted according to least favorable distributions resulting from a distributionally robust problem. As shown in the theoretical results and demonstrated by experiments, our methods achieve outstanding performance in classification accuracy compared with other baselines using minimal resources. The robust classifier layer (9) serves an alternative to the usual softmax layer in a neural network for classification, and we believe it is promising for other machine learning tasks.

References

[1] Soroosh Shafieezadeh Abadeh, Peyman Mohajerin Mohajerin Esfahani, and Daniel Kuhn. Distributionally robust logistic regression. In *Advances in Neural Information Processing Systems*, pages 1576–1584, 2015.

[2] Akshay Agrawal, Brandon Amos, Shane Barratt, Stephen Boyd, Steven Diamond, and J Zico Kolter. Differentiable convex optimization layers. In *Advances in Neural Information Processing Systems*, pages 9558–9570, 2019.

[3] Naomi S. Altman. An introduction to kernel and nearest-neighbor nonparametric regression. *The American Statistician*, 46(3):175–185, 1992.

[4] Brandon Amos and J Zico Kolter. Optnet: Differentiable optimization as a layer in neural networks. In *Proceedings of the 34th International Conference on Machine Learning-Volume 70*, pages 136–145. JMLR. org, 2017.

[5] Guilherme Aresta, Teresa Araújo, Scotty Kwok, Sai Saketh Chennamsetty, Mohammed Safwan, Varghese Alex, Bahram Marami, Marcel Prastawa, Monica Chan, Michael Donovan, Gerardo

Fernandez, Jack Zeineh, Matthias Kohl, Christoph Walz, Florian Ludwig, Stefan Braunewell, Maximilian Baust, Quoc Dang Vu, Minh Nguyen Nhat To, Eal Kim, Jin Tae Kwak, Sameh Galal, Veronica Sanchez-Freire, Nadia Brancati, Maria Frucci, Daniel Riccio, Yaqi Wang, Lingling Sun, Kaiqiang Ma, Jiannan Fang, Ismael Kone, Lahsen Boulmane, Aurélio Campilho, Catarina Eloy, António Polónia, and Paulo Aguiar. Bach: Grand challenge on breast cancer histology images. *Medical Image Analysis*, 56:122 – 139, 2019.

[6] Jose Blanchet, Yang Kang, and Karthyek Murthy. Robust Wasserstein profile inference and applications to machine learning. *Journal of Applied Probability*, 56(3):830–857, 2019.

[7] Jose Blanchet, Yang Kang, Fan Zhang, Fei He, and Zhangyi Hu. Doubly robust data-driven distributionally robust optimization. *arXiv preprint arXiv:1705.07168*, 2017.

[8] Jose Blanchet and Karthyek Murthy. Quantifying distributional model risk via optimal transport. *Mathematics of Operations Research*, 44(2):565–600, 2019.

[9] Ruidi Chen and Ioannis Paschalidis. Selecting optimal decisions via distributionally robust nearest-neighbor regression. In H. Wallach, H. Larochelle, A. Beygelzimer, F. dAlché Buc, E. Fox, and R. Garnett, editors, *Advances in Neural Information Processing Systems 32*, pages 749–759. Curran Associates, Inc., 2019.

[10] Ruidi Chen, Ioannis Ch Paschalidis, et al. Distributionally robust learning. *Foundations and Trends® in Optimization*, 4(1-2):1–243, 2020.

[11] Thomas M. Cover and Joy A. Thomas. *Elements of Information Theory (Wiley Series in Telecommunications and Signal Processing)*. Wiley-Interscience, USA, 2006.

[12] Dheeru Dua and Casey Graff. UCI machine learning repository: Lung cancer data set, 2017.

[13] Peyman Mohajerin Esfahani and Daniel Kuhn. Data-driven distributionally robust optimization using the Wasserstein metric: Performance guarantees and tractable reformulations. *Mathematical Programming*, 171(1-2):115–166, 2018.

[14] Farzan Farnia and David Tse. A minimax approach to supervised learning. In D. Lee, M. Sugiyama, U. Luxburg, I. Guyon, and R. Garnett, editors, *Advances in Neural Information Processing Systems*, volume 29. Curran Associates, Inc., 2016.

[15] Chelsea Finn, Pieter Abbeel, and Sergey Levine. Model-agnostic meta-learning for fast adaptation of deep networks. In Doina Precup and Yee Whye Teh, editors, *Proceedings of the 34th International Conference on Machine Learning*, volume 70 of *Proceedings of Machine Learning Research*, pages 1126–1135, International Convention Centre, Sydney, Australia, 06–11 Aug 2017. PMLR.

[16] Rui Gao, Xi Chen, and Anton J Kleywegt. Wasserstein distributional robustness and regularization in statistical learning. *arXiv preprint arXiv:1712.06050*, 2017.

[17] Rui Gao and Anton J Kleywegt. Distributionally robust stochastic optimization with Wasserstein distance. *arXiv preprint arXiv:1604.02199*, 2016.

[18] Rui Gao, Liyan Xie, Yao Xie, and Huan Xu. Robust hypothesis testing using Wasserstein uncertainty sets. In *Proceedings of the 32nd International Conference on Neural Information Processing Systems*, NIPS'18, page 7913–7923, Red Hook, NY, USA, 2018. Curran Associates Inc.

[19] Jacob Goldberger, Geoffrey E Hinton, Sam T. Roweis, and Russ R Salakhutdinov. Neighbourhood components analysis. In L. K. Saul, Y. Weiss, and L. Bottou, editors, *Advances in Neural Information Processing Systems 17*, pages 513–520. MIT Press, 2005.

[20] Lee-Ad Gottlieb, Aryeh Kontorovich, and Robert Krauthgamer. Efficient classification for metric data. *IEEE Transactions on Information Theory*, 60(9):5750–5759, 2014.

[21] Peter J Huber. A robust version of the probability ratio test. *Annals of Mathematical Statistics*, 36(6):1753–1758, 1965.

[22] Wen Jiang, Kai Huang, Jie Geng, and Xinyang Deng. Multi-scale metric learning for few-shot learning. *IEEE Transactions on Circuits and Systems for Video Technology*, 31(3):1091–1102, 2021.

[23] Diederik P Kingma and Jimmy Ba. Adam: A method for stochastic optimization. *arXiv preprint arXiv:1412.6980*, 2014.

[24] Gregory Koch, Richard Zemel, and Ruslan Salakhutdinov. Siamese neural networks for one-shot image recognition. In *ICML deep learning workshop*, volume 2. Lille, 2015.

[25] Alex Krizhevsky, Vinod Nair, and Geoffrey Hinton. Cifar-10 (canadian institute for advanced research). 2020.

[26] Daniel Kuhn, Peyman Mohajerin Esfahani, Viet Anh Nguyen, and Soroosh Shafieezadeh-Abadeh. Wasserstein distributionally robust optimization: Theory and applications in machine learning. In *Operations Research & Management Science in the Age of Analytics*, pages 130–166. INFORMS, 2019.

[27] Brenden M Lake, Ruslan Salakhutdinov, and Joshua B Tenenbaum. Human-level concept learning through probabilistic program induction. *Science*, 350(6266):1332–1338, 2015.

[28] Yann LeCun and Corinna Cortes. MNIST handwritten digit database. 2010.

[29] Kwonjoon Lee, Subhransu Maji, Avinash Ravichandran, and Stefano Soatto. Meta-learning with differentiable convex optimization. In *Proceedings of the IEEE Conference on Computer Vision and Pattern Recognition*, pages 10657–10665, 2019.

[30] Fei-Fei Li, R. Fergus, and P. Perona. One-shot learning of object categories. *IEEE Transactions on Pattern Analysis and Machine Intelligence*, 28(4):594–611, 2006.

[31] Xiaoxu Li, Xiaochen Yang, Zhanyu Ma, and Jing-Hao Xue. Deep metric learning for few-shot image classification: A selective review. *arXiv preprint arXiv:2105.08149*, 2021.

[32] Tingting Liao, Zhen Lei, Tianqing Zhu, Shan Zeng, Yaqin Li, and Cao Yuan. Deep metric learning for k nearest neighbor classication. *IEEE Transactions on Knowledge and Data Engineering*, 2021.

[33] Tobias Plötz and Stefan Roth. Neural nearest neighbors networks. In *Proceedings of the 32nd International Conference on Neural Information Processing Systems*, NIPS'18, page 1095–1106, Red Hook, NY, USA, 2018. Curran Associates Inc.

[34] Ruslan Salakhutdinov and Geoff Hinton. Learning a nonlinear embedding by preserving class neighbourhood structure. In Marina Meila and Xiaotong Shen, editors, *Proceedings of the Eleventh International Conference on Artificial Intelligence and Statistics*, volume 2 of *Proceedings of Machine Learning Research*, pages 412–419, San Juan, Puerto Rico, 21–24 Mar 2007. PMLR.

[35] Richard J Samworth. Optimal weighted nearest neighbour classifiers. *The Annals of Statistics*, 40(5):2733–2763, 2012.

[36] Soroosh Shafieezadeh-Abadeh, Daniel Kuhn, and Peyman Mohajerin Esfahani. Regularization via mass transportation. *Journal of Machine Learning Research*, 20(103):1–68, 2019.

[37] Alexander Shapiro, Darinka Dentcheva, and Andrzej Ruszczyński. *Lectures on stochastic programming: modeling and theory*. SIAM, 2014.

[38] Aman Sinha, Hongseok Namkoong, and John Duchi. Certifying some distributional robustness with principled adversarial training. *arXiv preprint arXiv:1710.10571*, 2017.

[39] Jake Snell, Kevin Swersky, and Richard Zemel. Prototypical networks for few-shot learning. In I. Guyon, U. V. Luxburg, S. Bengio, H. Wallach, R. Fergus, S. Vishwanathan, and R. Garnett, editors, *Advances in Neural Information Processing Systems 30*, pages 4077–4087. Curran Associates, Inc., 2017.

[40] Cédric Villani. *Optimal transport: old and new*, volume 338. Springer Science & Business Media, 2008.

[41] Oriol Vinyals, Charles Blundell, Timothy Lillicrap, Koray Kavukcuoglu, and Daan Wierstra. Matching networks for one shot learning. In *Proceedings of the 30th International Conference on Neural Information Processing Systems*, NIPS'16, page 3637–3645, Red Hook, NY, USA, 2016. Curran Associates Inc.

[42] Ulrike von Luxburg and Olivier Bousquet. Distance-based classification with lipschitz functions. *J. Mach. Learn. Res.*, 5(Jun):669–695, 2004.

[43] Yaqing Wang, Quanming Yao, James Kwok, and Lionel M. Ni. Generalizing from a few examples: A survey on few-shot learning, 2019.

[44] Xingyi Yang, Xuehai He, Jinyu Zhao, Yichen Zhang, Shanghang Zhang, and Pengtao Xie. COVID-CT-Dataset: A CT scan dataset about COVID-19, 2020.

Checklist

1. For all authors...
   (a) Do the main claims made in the abstract and introduction accurately reflect the paper's contributions and scope? [Yes]
   (b) Did you describe the limitations of your work? [Yes] See Section 6
   (c) Did you discuss any potential negative societal impacts of your work? [N/A]
   (d) Have you read the ethics review guidelines and ensured that your paper conforms to them? [Yes]
2. If you are including theoretical results...
   (a) Did you state the full set of assumptions of all theoretical results? [Yes]
   (b) Did you include complete proofs of all theoretical results? [Yes]
3. If you ran experiments...
   (a) Did you include the code, data, and instructions needed to reproduce the main experimental results (either in the supplemental material or as a URL)? [Yes]
   (b) Did you specify all the training details (e.g., data splits, hyperparameters, how they were chosen)? [Yes]
   (c) Did you report error bars (e.g., with respect to the random seed after running experiments multiple times)? [N/A]
   (d) Did you include the total amount of compute and the type of resources used (e.g., type of GPUs, internal cluster, or cloud provider)? [Yes]
4. If you are using existing assets (e.g., code, data, models) or curating/releasing new assets...
   (a) If your work uses existing assets, did you cite the creators? [Yes]
   (b) Did you mention the license of the assets? [N/A]
   (c) Did you include any new assets either in the supplemental material or as a URL? [Yes]
   (d) Did you discuss whether and how consent was obtained from people whose data you're using/curating? [N/A]
   (e) Did you discuss whether the data you are using/curating contains personally identifiable information or offensive content? [Yes]
5. If you used crowdsourcing or conducted research with human subjects...
   (a) Did you include the full text of instructions given to participants and screenshots, if applicable? [N/A]
   (b) Did you describe any potential participant risks, with links to Institutional Review Board (IRB) approvals, if applicable? [N/A]
   (c) Did you include the estimated hourly wage paid to participants and the total amount spent on participant compensation? [N/A]

A Learning Algorithm

Algorithm 1: Learning algorithm for `Dr.k-NN`

Input: $S_m := \{(x^i, y^i) : y^i = m, \forall i\} \subset S,\ m = 1, \dots, M$;
Output: The feature mapping $\phi(\cdot;\theta)$ and the LFD $P_1^*, \dots, P_M^*$ supported on training samples;
Initialization: θ_0 is randomly initialized; $n' < n$ is the size of "mini-set"; $t = 0$;
while $t < T$ **do**
  for *number of mini-sets* **do**
    Randomly generate M integers $n_1, \dots, n_M$ such that $\sum_{m=1}^M n_m = n', n_m > 0, \forall m$;
    Initialize two ordered sets $\widehat{\Xi} = \emptyset, \widehat{P} = \emptyset$;
    for $m \in \{1, \dots, M\}$ **do**
      $\mathcal{X}_m \leftarrow$ Randomly sample n_m points from S_m;
      $\widehat{\Xi}_m \leftarrow \{\xi := \phi(x;\theta_t) : x \in \mathcal{X}_m\}$;
      $\widehat{P}_m \leftarrow \frac{1}{n_m}\sum_{i=1}^{n_m} \delta_{\xi_m^i},\ \xi_m^i \in \widehat{\Xi}_m$;
      $\widehat{\Xi} \leftarrow \widehat{\Xi} \cup \widehat{\Xi}_m$; $\widehat{P} \leftarrow \widehat{P} \cup \widehat{P}_m$;
    end
    Update the probability mass of LFDs $P_1^*, \dots, P_M^*$ on $\widehat{\Xi}$ by solving (9) given $\widehat{\Xi}, \widehat{P}$;
  end
  $\theta_{t+1} \leftarrow \theta_t - \alpha \nabla J(\theta_t; P_1^*, \dots, P_M^*)$, where α is the learning rate;
  $t \leftarrow t + 1$;
end

B Proofs for Section 3

B.1 Proof of Theorem 1

The proof of Theorem 1 is based on the following two lemmas.

Lemma 1. *Fix probability distributions $P_1, \dots, P_M \in \mathscr{P}(\widehat{\Xi})$, where $\widehat{\Xi} = \{\xi^1, \dots, \xi^n\}$. Then*

$$\psi(P_1, \dots, P_M) := \min_{\pi : \widehat{\Xi} \to \Delta_M} \Psi(\pi; P_1, \dots, P_M) = M - \sum_{i=1}^n \max_{1 \le m \le M} P_m(\xi^i).$$

Furthermore, the optimal classifier π^* satisfies that for any $\xi^i \in \widehat{\Xi}$,

$$\big\{m : \pi_m^*(\xi^i) > 0, 1 \le m \le M\big\} \subset \operatorname*{arg\,max}_{1 \le m \le M} \frac{P_m(\xi^i)}{\sum_{m=1}^M P_m(\xi^i)}.$$

This lemma gives a closed-form expression for the risk of the optimal classifier if $P_1, \dots, P_M$ are known, and shows that the optimal decision π^* accepts the class with the maximum likelihood. Moreover, when there is a tie (i.e., the set $\arg\max_{1 \le m \le M} P_m(\xi)$ is not singleton), the optimal decision π^* can break the tie arbitrarily.

Proof of Lemma 1. We here prove a more general result for an arbitrary sample space Ξ. Note that each P_m, $1 \le m \le M$, is absolutely continuous with respect to $P_1 + \cdots + P_M$, hence the Radon-Nikodym derivative $\frac{dP_m}{d(P_1 + \cdots + P_M)}$ exists. Using the interchangeability principle [37] that enables us to exchange the minimization and integration, we have

$$\begin{aligned}
\min_{\pi : \Xi \to \Delta_M} \Psi(\pi; P_1, \dots, P_M) &= \min_{\pi : \Xi \to \Delta_M} \int_\Xi \Big[\sum_{m=1}^M (1 - \pi_m(\xi)) \tfrac{dP_m}{d(P_1 + \cdots + P_M)}(\xi) \Big] d(P_1 + \cdots + P_M) \\
&= \int_\Xi \min_{\pi \in \Delta_M} \Big[\sum_{m=1}^M (1 - \pi_m) \tfrac{dP_m}{d(P_1 + \cdots + P_M)}(\xi) \Big] d(P_1 + \cdots + P_M) \\
&= \int_\Xi \Big[1 - \max_{1 \le m \le M} \tfrac{dP_m}{d(P_1 + \cdots + P_M)}(\xi) \Big] d(P_1 + \cdots + P_M),
\end{aligned} \tag{14}$$

where the first equality is obtained by plugging in the definition of Ψ in (1); the second equality is due the interchangeability principle; and the last equality holds because for any ξ, the inner minimization attains its minimum at one of the vertices of Δ_M. More specifically, note that for each ξ, the objective of the inner minimization problem equals to $1 - \sum_{m=1}^{M} \pi_m \frac{dP_m}{d(P_1+\cdots+P_M)}(\xi)$. Under the constaint that $\pi \in \Delta_M$, i.e., $\sum_{m=1}^{M} \pi_m = 1$, we have:

$$\sum_{m=1}^{M} \pi_m \frac{dP_m}{d(P_1+\cdots+P_M)}(\xi) \leq \max_{1\leq m\leq M} \frac{dP_m}{d(P_1+\cdots+P_M)}(\xi),$$

and the equality holds when π are chosen such that

$$\{m : \pi_m > 0, 1 \leq m \leq M\} \subset \arg\max_{1\leq m\leq M} \frac{dP_m(\xi)}{\sum_{m=1}^{M} dP_m(\xi)}.$$

If there is a single maximum in $\{\frac{dP_m}{d(P_1+\cdots+P_M)}(\xi), 1 \leq m \leq M\}$, say at index m^*, then this simply implies that the optimal π is chosen as $\pi_{m^*} = 1$ and $\pi_m = 0$ for $m \neq m^*$.

If we substitute Ξ with the empirical support $\widehat{\Xi}$, the above formulation in Equation (14) translates into

$$\min_{\pi:\widehat{\Xi}\to\Delta_M} \Psi(\pi; P_1, \ldots, P_M) = M - \sum_{i=1}^{n} \max_{1\leq m\leq M} P_m(\xi^i),$$

therefore the lemma is proved. □

Lemma 2. *For the uncertainty sets defined in* (7)*, the problem* $\max_{P_m\in\mathcal{P}_m, 1\leq m\leq M}\ \psi(P_1, \ldots, P_M)$ *is equivalent to* (9)*.*

Proof of Lemma 2. Recall that the Wasserstein metric of order 1 is defined as

$$\mathcal{W}(P, P') := \min_{\gamma}\ \mathbb{E}_{(\xi,\xi')\sim\gamma}\left[c(\xi, \xi')\right]$$

for any two distributions P and P' on Ξ, where the minimization of γ is taken over the set of all probability distributions on $\Xi \times \Xi$ with marginals P and P', i.e., the set

$$\left\{\gamma \in \mathscr{P}(\Xi \times \Xi) : \int_{\Xi} \gamma(\xi, \xi')d\xi' = P(\xi), \int_{\Xi} \gamma(\xi, \xi')d\xi = P'(\xi'), \forall \xi, \xi' \in \Xi\right\},$$

where $\mathscr{P}(\Xi \times \Xi)$ denotes the joint probability distributions on $\Xi \times \Xi$. Therefore, the Wasserstein metric $\mathcal{W}(P, P')$ can be rewritten as

$$\min_{\gamma}\left\{\int_{\Xi\times\Xi} c(\xi, \xi')\gamma(\xi, \xi')d\xi d\xi' : \int_{\Xi} \gamma(\xi, \xi')d\xi' = P(\xi), \int_{\Xi} \gamma(\xi, \xi')d\xi = P'(\xi'), \forall \xi, \xi' \in \Xi\right\}$$

By the definition of uncertainty sets in (7) which contains discrete distributions supported on $\widehat{\Xi}$, we can introduce additional variables $\gamma_m \in \mathbb{R}_+^{n\times n}$ which represents the distribution on $\widehat{\Xi} \times \widehat{\Xi}$, with marginals $P_m \in \mathcal{P}_m$ and $\widehat{P}_m$, for $1 \leq m \leq M$. For any $\xi^i, \xi^j \in \widehat{\Xi}$, let $\gamma_m^{i,j}$ denotes $\gamma_m(\xi^i, \xi^j)$ for simplicity. Thus the objective function in the above reformualtion of $\mathcal{W}(P_m, \widehat{P}_m)$ is $\sum_{i=1}^{n}\sum_{j=1}^{n} \gamma_m^{i,j} c(\xi^i, \xi^j)$. The constraints $\mathcal{W}(P_m, \widehat{P}_m) \leq \vartheta_m$ in (7) can be rewritten using γ_m as

$$\sum_{i=1}^{n}\sum_{j=1}^{n} \gamma_m^{i,j} c(\xi^i, \xi^j) \leq \vartheta_m, \quad m = 1, \ldots, M.$$

Furthermore, the marginal distribution constraint of γ_m reads:

$$\sum_{i=1}^{n} \gamma_m^{i,j} = \widehat{P}_m(\xi^j), \quad \sum_{j=1}^{n} \gamma_m^{i,j} = P_m(\xi^i), \quad m = 1, \ldots, M.$$

Thereby the problem $\max_{P_m\in\mathcal{P}_m, 1\leq m\leq M}\ \psi(P_1, \ldots, P_M)$ is equivalent to the convex optimization formulation in (9). □

Proof to Theorem 1. By Lemmas 1 and 2, we have

$$\max_{P_m\in\mathcal{P}_m,1\le m\le M}\ \min_{\pi:\widehat{\Xi}\to\Delta_M}\Psi(\pi;P_1,\dots,P_M)=\max_{P_m\in\mathcal{P}_m,1\le m\le M}\psi(P_1,\dots,P_M)=(9).$$

To prove Theorem 1, it remains to verify the validity of exchanging $\max$ and $\min$. We identify π as $(\pi^1,\dots,\pi^n)$, where $\pi^i\in\mathbb{R}_+^M$ satisfies $\sum_{m=1}^M\pi_m^i=1$. Similar to the proof of Lemma 2, P_m, $1\le m\le M$, can also be identified as a vector in $\mathbb{R}^n$. Note that the objective function $\Psi(\pi;P_1,\dots,P_M)$ is linear in $(\pi^1,\dots,\pi^n)$ and concave in $(P_1,\dots,P_M)$, and the Slater condition holds. Hence applying convex programming duality we can exchange $\max$ and $\min$ and thus the result follows. It is worth mentioning that the optimal solution π^* and corresponding LFDs $P_1^*,\dots,P_M^*$ always exist since they are solutions to a saddle point problem. □

B.2 Proof of Theorem 2

Proof of Theorem 2. On the one hand, since $\pi^{\mathsf{knn}}(\cdot;k,w)$ can be regarded as a special case of the general classifier $\pi:\Xi\to\Delta_M$, it holds that

$$\begin{aligned}&\min_{\substack{w_m:\Xi\times\Xi\to\mathbb{R}_+,\,1\le m\le M\\1\le k\le n}}\ \max_{P_m\in\mathcal{P}_m,1\le m\le M}\sum_{m=1}^M\mathbb{E}_{\xi_m\sim P_m}[1-\pi_m^{\mathsf{knn}}(\xi_m;k,w)]\\ \ge&\min_{\pi:\widehat{\Xi}\to\Delta_M}\ \max_{P_m\in\mathcal{P}_m,1\le m\le M}\sum_{m=1}^M\mathbb{E}_{\xi_m\sim P_m}[1-\pi_m(\xi_m)].\end{aligned}$$

On the other hand, by Lemma 2, there exists an optimal solution to the minimax problem (8), denoted as $(P_1^*,\dots,P_M^*)$, and the optimal classifier π^* as given in Lemma 1. Note that there exists $1\le k^*\le n$ and weight functions $w_1^*,\dots,w_M^*$ such that

$$\pi_m^{\mathsf{knn}}(\xi;k^*,w^*)=\pi_m^*(\xi),\quad\forall\xi\in\widehat{\Xi},\tag{15}$$

for example, by taking $k^*=1$ and $w_m^*=P_m^*$, $1\le m\le M$. This implies that

$$\begin{aligned}&\min_{\substack{w_m:\Xi\times\Xi\to\mathbb{R}_+,\,1\le m\le M\\1\le k\le K}}\ \max_{P_m\in\mathcal{P}_m,1\le m\le M}\sum_{m=1}^M\mathbb{E}_{\xi_m\sim P_m}[1-\pi_m^{\mathsf{knn}}(\xi_m;k,w)]\\ \le&\max_{P_m\in\mathcal{P}_m,1\le m\le M}\sum_{m=1}^M\mathbb{E}_{\xi_m\sim P_m}[1-\pi_m^{\mathsf{knn}}(\xi_m;k^*,w^*)]\\ =&\max_{P_m\in\mathcal{P}_m,1\le m\le M}\sum_{m=1}^M\mathbb{E}_{\xi_m\sim P_m}[1-\pi_m^*(\xi_m)]\\ =&\min_{\pi:\widehat{\Xi}\to\Delta_M}\ \max_{P_m\in\mathcal{P}_m,1\le m\le M}\sum_{m=1}^M\mathbb{E}_{\xi_m\sim P_m}[1-\pi_m(\xi_m)].\end{aligned}$$

Thereby we have shown that formulations (6) and (8) have identical optimal values. Moreover, by the strong duality results in Theorem 1, we know $(\pi^*;P_1^*,\dots,P_M^*)$ is the saddle point for the formulation (8), and by the above arguments, we see that $(\pi^{\mathsf{knn}};P_1^*,\dots,P_M^*)$ leads to the same optimal value for formulation (6) as $(\pi^*;P_1^*,\dots,P_M^*)$ for formulation (8). Therefore, we show that π^{knn} is indeed the optimal solution to (6). □

B.3 Proof of Theorem 3

Proof of Theorem 3. We first show the equivalence between the Lipschitz regularized problem (11) and the minimax problem (8). Denote by v_{Lip} the optimal value of (11) and v_{dual} the optimal value of (10).

Observe that if $\|\pi_m\|_{\text{Lip}}\le\lambda_m$, then

$$\max_{\xi\in\widehat{\Xi}}\left\{1-\pi_m(\xi)-\lambda_m c(\xi,\widehat{\xi})\right\}=1-\pi_m(\hat{\xi}),\ \forall\hat{\xi}\in\widehat{\Xi}.$$

Therefore, we have

$$
\begin{aligned}
v_{\text{dual}} \leq & \min_{\pi:\, \widehat{\Xi}\to\Delta_M,\ (\lambda_m)_{1\leq m\leq M}\geq 0,\ \|\pi_m\|_{\text{Lip}}\leq\lambda_m} \left\{ \sum_{m=1}^{M} \lambda_m \vartheta_m + \mathbb{E}_{\hat{\xi}\sim\widehat{P}_m} \left[\max_{\xi\in\widehat{\Xi}} \left\{ 1-\pi_m(\xi)-\lambda_m c(\xi,\hat{\xi}) \right\} \right] \right\} \\
= & \min_{\pi:\, \widehat{\Xi}\to\Delta_M} \left\{ \sum_{m=1}^{M} \|\pi_m\|_{\text{Lip}} \vartheta_m + \mathbb{E}_{\hat{\xi}\sim\widehat{P}_m} \left[1-\pi_m(\hat{\xi}) \right] \right\} \\
= & v_{\text{Lip}}.
\end{aligned}
$$

If we can show $v_{\text{dual}} \geq v_{\text{Lip}}$, then we prove the equivalence between (11) and (10), thus the equivalence between (11) and (8).

Let $(\pi^*; \lambda_1^*, \ldots, \lambda_M^*)$ be a dual minimizer of problem (10), whose existence is ensured by [17].

Define

$$
\phi_m(\xi) := \max_{\tilde{\xi}\in\widehat{\Xi}} \left\{ 1-\pi_m^*(\tilde{\xi})-\lambda_m^* c(\tilde{\xi},\xi) \right\}, \quad m=1,\ldots,M.
$$

Then it follows that

$$
\pi_m^*(\tilde{\xi}) \geq 1-\lambda_m^* c(\tilde{\xi},\xi)-\phi_m(\xi),\ \ \forall \xi,\tilde{\xi}\in\widehat{\Xi},\ m=1,\ldots,M.
$$

Define

$$
\tilde{\pi}_m(\tilde{\xi}) := \max_{\xi\in\widehat{\Xi}} \{ 1-\lambda_m^* c(\xi,\tilde{\xi})-\phi_m(\xi) \}, \quad m=1,\ldots,M.
$$

Then by definition, $\|\tilde{\pi}_m\|_{\text{Lip}} \leq \lambda_m^*$. Indeed, for any $\xi,\tilde{\xi}\in\widehat{\Xi}$, there exists a $\xi_0 \in \arg\max_{\hat{\xi}\in\widehat{\Xi}} \{1-\lambda_m^* c(\hat{\xi},\xi)-\phi_m(\hat{\xi})\}$ such that:

$$
\begin{aligned}
\tilde{\pi}_m(\xi)-\tilde{\pi}_m(\tilde{\xi}) = & 1-\lambda_m^* c(\xi_0,\xi)-\phi_m(\xi_0)-\tilde{\pi}_m(\tilde{\xi}) \\
\leq & [1-\lambda_m^* c(\xi_0,\xi)-\phi_m(\xi_0)]-[1-\lambda_m^* c(\xi_0,\tilde{\xi})-\phi_m(\xi_0)] \\
= & \lambda_m^* c(\xi_0,\tilde{\xi})-\lambda_m^* c(\xi_0,\xi) \\
\leq & \lambda_m^* c(\xi,\tilde{\xi}).
\end{aligned}
$$

Furthermore, since $\tilde{\pi}_m(\tilde{\xi}) \geq 1-\lambda_m^* c(\xi,\tilde{\xi})-\phi_m(\xi)$, $\forall \xi,\tilde{\xi}$, we have $\phi_m(\xi) \geq 1-\tilde{\pi}_m(\tilde{\xi})-\lambda_m^* c(\xi,\tilde{\xi})$, $\forall \tilde{\xi}\in\widehat{\Xi}$. Hence, we have $\phi_m(\xi) \geq \max_{\tilde{\xi}\in\widehat{\Xi}} \left\{ 1-\tilde{\pi}_m(\tilde{\xi})-\lambda_m^* c(\xi,\tilde{\xi}) \right\}$. Recall that $(\pi^*; \lambda_1^*, \ldots, \lambda_M^*)$ is a dual minimizer of problem (10):

$$
v_{\text{dual}} := \sum_{m=1}^{M} \lambda_m^* \vartheta_m + \mathbb{E}_{\hat{\xi}\sim\widehat{P}_m} \left[\max_{\xi\in\widehat{\Xi}} \left\{ 1-\pi_m^*(\xi)-\lambda_m^* c(\xi,\hat{\xi}) \right\} \right] = \sum_{m=1}^{M} \lambda_m^* \vartheta_m + \mathbb{E}_{\hat{\xi}\sim\widehat{P}_m} \left[\phi_m(\hat{\xi}) \right],
$$

thus

$$
v_{\text{dual}} \geq \sum_{m=1}^{M} \lambda_m^* \vartheta_m + \mathbb{E}_{\hat{\xi}\sim\widehat{P}_m} \left[\max_{\xi\in\widehat{\Xi}} \left\{ 1-\tilde{\pi}_m(\xi)-\lambda_m^* c(\xi,\hat{\xi}) \right\} \right] = \sum_{m=1}^{M} \lambda_m^* \vartheta_m + \mathbb{E}_{\hat{\xi}\sim\widehat{P}_m} \left[1-\tilde{\pi}_m(\hat{\xi}) \right].
$$

Since v_{dual} is the minimum value, this means that if $\tilde{\pi}$ is a feasible solution, then it is also an optimal solution to (10).

Next we verify $\tilde{\pi}$ is a feasible classifier, i.e., it satisfies $0 \leq \tilde{\pi}(\xi) \leq 1$ and $\sum_{m=1}^{M} \tilde{\pi}_m(\xi) = 1, \forall \xi$. First, by definition, $\pi_m^*(\tilde{\xi}) \geq \tilde{\pi}_m(\tilde{\xi})$, $\forall \tilde{\xi}\in\widehat{\Xi}$, therefore $\tilde{\pi}_m(\tilde{\xi}) \leq 1$ and $\sum_{m=1}^{M} \tilde{\pi}_m(\tilde{\xi}) \leq 1$. If we are able to show that

$$
\sum_{m=1}^{M} \tilde{\pi}_m(\tilde{\xi}) \geq 1,\ \ \forall \tilde{\xi}\in\widehat{\Xi}, \tag{16}
$$

then we can show $\tilde{\pi}$ is indeed a feasible classifier.

To show (16), first note that if $\pi_m^*(\tilde{\xi}) = 0$, then we have by definition $\tilde{\pi}_m(\tilde{\xi}) = 0$. Moreover, for any $\tilde{\xi}\in\widehat{\Xi}$, there is a set $\mathcal{M}_0 \subset \{1,\ldots,M\}$ such that for all $m\in\mathcal{M}_0$, $\pi_m^*(\tilde{\xi}) > 0$, and the worst-case

distribution P_m^* transports probability mass from $\operatorname{supp} \widehat{P}_m$ to $\tilde{\xi}$, which suggests that there exits $\hat{\xi}_m \in \operatorname{supp} \widehat{P}_m$ such that

$$\tilde{\xi} \in \arg\max_{\xi \in \widehat{\Xi}} \{1 - \pi_m^*(\xi) - \lambda_m^* c(\xi, \hat{\xi}_m)\}.$$

It follows from the definition of ϕ_m that

$$\sum_{m \in \mathcal{M}_0} \phi_m(\hat{\xi}_m) = \sum_{m \in \mathcal{M}_0} \left(1 - \pi_m^*(\tilde{\xi}) - \lambda_m^* c(\tilde{\xi}, \hat{\xi}_m)\right).$$

Meanwhile, by definition of $\tilde{\pi}_m$,

$$\sum_{m \in \mathcal{M}_0} \tilde{\pi}_m(\tilde{\xi}) \geq \sum_{m \in \mathcal{M}_0} \left(1 - \lambda_m^* c(\tilde{\xi}, \hat{\xi}_m) - \phi_m(\hat{\xi}_m)\right) = \sum_{m \in \mathcal{M}_0} \pi_m^*(\tilde{\xi}) = 1.$$

Thereby we have shown (16). The proof is completed by noting that the optimal solution $\tilde{\pi}$ satisfies $\|\tilde{\pi}_m\|_{\text{Lip}} \leq \lambda_m^*$ and thus $v_{\text{dual}} \geq v_{\text{Lip}}$. Combine with the previous result that $v_{\text{dual}} \leq v_{\text{Lip}}$, we have shown $v_{\text{dual}} = v_{\text{Lip}}$ and the proof is completed.

□

C Memory-efficient implementation of `Dr.k-NN` in data-intensive scenario

For the sake of completeness, we extend our algorithm to non-few-training-sample setting. This can be particularly useful for the general classification problem with an arbitrary size of training set. In fact, k-NN methods notoriously suffer from computational inefficiency if the number of labeled samples n is large, since it has to store and search through the entire training set [19].

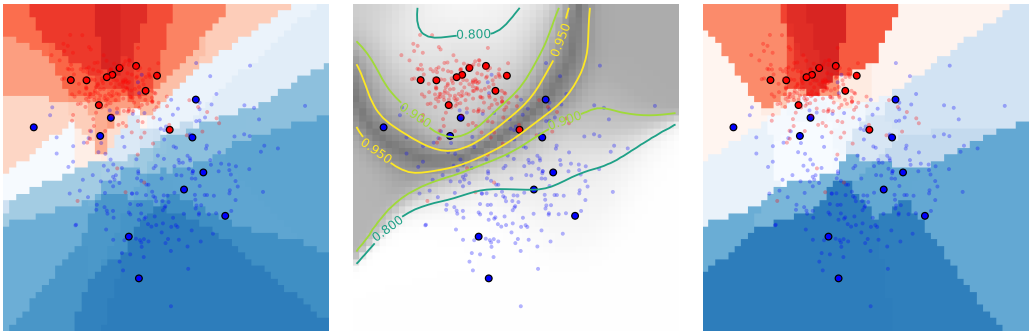

(a) `Dr.k-NN` (b) τ-truncated set (c) Truncated

Figure 6: An example of the truncated `Dr.k-NN` using MNIST (digit 4 (red) and 9 (blue)). Big dots represent training samples and small dots represent query samples. (a) shows the decision made by `Dr.k-NN`; (c) shows the decision made by the truncated `Dr.k-NN` with truncation level $\tau = 0.9$; (b) shows τ-truncated regions with $\tau = 0.95, 0.9, 0.8$. Big dots between the lines are selected training samples under different τ. The depth of the shaded area shows the level of samples entropy.

The main idea is to only keep the training samples that are important in deciding the decision boundary based on the maximum entropy principle [11]. As a measure of importance, we choose the samples with the largest entropy across all categories, based on the intuition that the samples with higher entropy has larger uncertainty and will be more useful for classification purposes since they tend to lie on the decision boundary. The entropy of a sample is defined as follows. Consider a random variable which takes value m with probability π_m, $\sum_{i=1}^M \pi_m = 1$; then the entropy of this random variable is define as

$$H(\pi_1, \ldots, \pi_M) = -\sum_{m=1}^M \pi_m \log \pi_m.$$

As a simple example, for Bernoulli random variable (which can represent, e.g., the outcome for flipping a coin with bias p), the entropy function is $H(p) = -p \log p - (1-p)\log(1-p)$, and it

is a concave function achieving the maximum at $p^* = 1/2$, which means that the fair-coin has the maximum entropy; this is intuitive as indeed the outcome of a fair coin toss is the most difficult to predict. Now we use this entropy to define the "uncertainty" associated with each training points. With a little abuse of notation, define

$$H(\widehat{\xi}) := H(\pi_1(\widehat{\xi}), \ldots, \pi_M(\widehat{\xi})).$$

Denote the minimal and maximal entropy of all the training points as

$$H_{\text{min}} = \min\{H(\widehat{\xi}), \widehat{\xi} \in \widehat{\Xi}\}, \quad H_{\text{max}} = \max\{H(\widehat{\xi}), \widehat{\xi} \in \widehat{\Xi}\}.$$

Define the τ-truncated training set as

$$\widetilde{\Xi} = \{\widehat{\xi} \in \widehat{\Xi} : (H(\widehat{\xi}) - H_{\text{min}})/(H_{\text{max}} - H_{\text{min}}) \geq \tau\}, \forall \tau \in [0, 1].$$

The truncated `Dr.k-NN` is obtained similarly as Step 2 of `Dr.k-NN` by restricting the training set $\widehat{\Xi}$ only to the samples in $\widetilde{\Xi}$ (samples with larger entropy). Figure 6 reveals that the most informative samples usually lie in between categories. We can see that a truncated `Dr.k-NN` classifier with $\tau = 0.9$ only uses 20% samples with little performance loss. More experimental details is presented in Section 5.

D Comparison to kernel smoothing

Figure 7 and Figure 8 present a comparison of the results using `Dr.k-NN` and the kernel smoothing defined in (13). The results suggest that the performance of `Dr.k-NN` is insensitive to the choice of k, while the performance of the kernel smoothing is heavily depended on the choice of h.

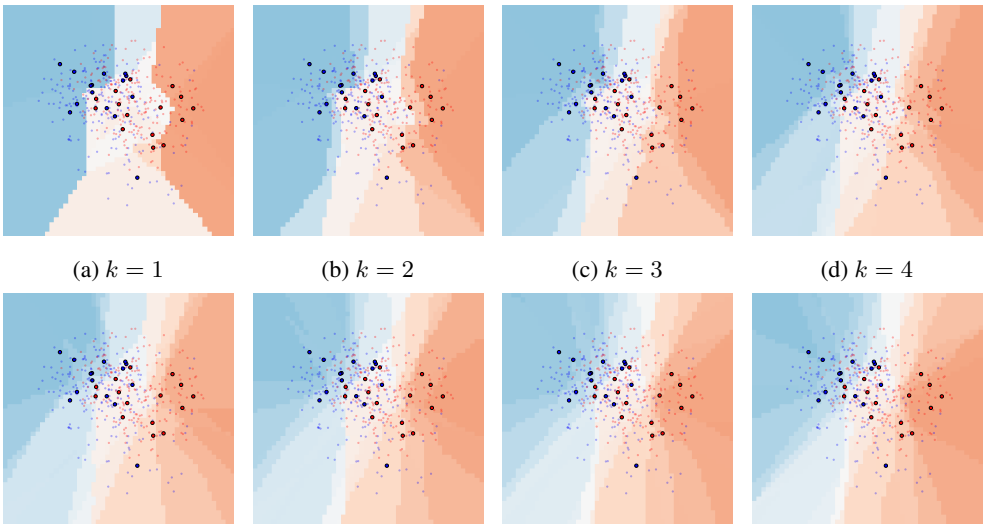

(a) $k = 1$ (b) $k = 2$ (c) $k = 3$ (d) $k = 4$

(e) $k = 5$ (f) $k = 6$ (g) $k = 7$ (h) $k = 8$

Figure 7: `Dr.k-NN` with different k.

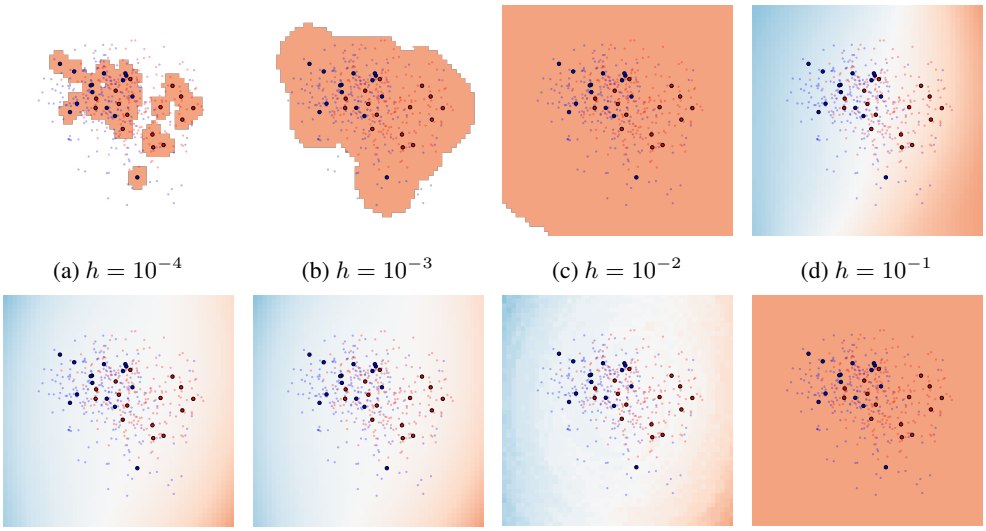

(a) $h = 10^{-4}$ (b) $h = 10^{-3}$ (c) $h = 10^{-2}$ (d) $h = 10^{-1}$

(e) $h = 1$ (f) $h = 10$ (g) $h = 10^{2}$ (h) $h = 10^{3}$

Figure 8: Kernel smoothing with different bandwidth h.

E Real data examples for COVID-19 CT

Figure 9 and Figure 10 show 16 real CT images collected from patients who have been diagnosed with COVID-19 and other diseases (non-COVID-19), respectively.

Figure 9: COVID-19 CT images.

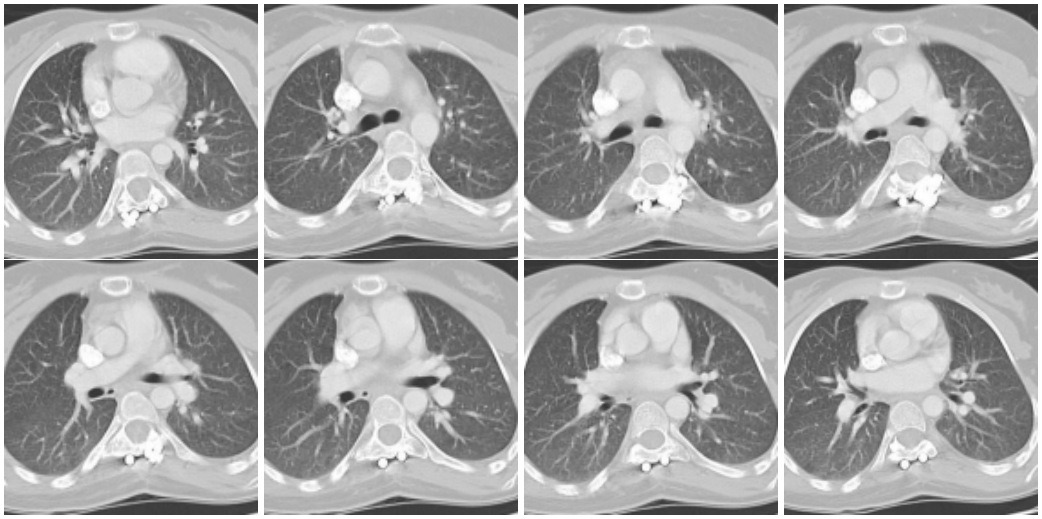

Figure 10: Non-COVID-19 CT images.